On the Computation of Eigen Modes for Lossy Microwave Transmission Lines Including Perfectly Matched Layer Boundary Conditions

G. Hebermehl [*] F. K. Hübner [†]
R. Schlundt [‡]

Weierstrass Institute for Applied Analysis and Stochastics, Mohrenstr. 39, D-10117 Berlin, Germany

T. Tischler [§] H. Zscheile [¶]
W. Heinrich [‖]

Ferdinand-Braun-Institut für Höchstfrequenztechnik, Albert-Einstein-Str. 11, D-12489 Berlin, Germany

December 17, 1999

1991 Mathematics Subject Classification.
35Q60, 65F15, 65N22.
Keywords.
Microwave device simulation, Maxwellian equations, PML boundary condition, finite-volume method, eigenvalue problem

[*]e-mail: hebermehl@wias-berlin.de, URL: http://www.wias-berlin.de
[†]e-mail: huebner@wias-berlin.de, URL: http://www.wias-berlin.de
[‡]e-mail: schlundt@wias-berlin.de, URL: http://www.wias-berlin.de
[§]e-mail: tischler@fbh-berlin.de, URL: http://www.fbh-berlin.de
[¶]e-mail: zscheile@fbh-berlin.de, URL: http://www.fbh-berlin.de
[‖]e-mail: heinrich@fbh-berlin.de, URL: http://www.fbh-berlin.de

Abstract

Design of microwave circuits requires detailed knowledge on the electromagnetic properties of the transmission lines used. This can be obtained by applying the Maxwellian equations to a longitudinally homogeneous waveguide structure, which results in an eigenvalue problem for the propagation constant. Using a finite-volume approach we get an algebraic formulation. In the presence of losses or absorbing boundary conditions its system matrix is complex. A method is presented which avoids the computation of all eigenvalues to find the few propagating modes one is interested in. Special attention is paid to the so-called Perfectly Matched Layer boundary conditions.

Contents

List of Figures

List of Tables

1 Introduction

The design of monolithic microwave integrated circuits (MMIC) requires efficient CAD tools in order to avoid costly and time-consuming redesign cycles. The fields of applications are mobile communications, radio links, sensors, and automobile systems. The commercial applications cover the microwave and lower millimeter-wave range, i.e., the frequencies between 1 GHz and about 80 GHz. For radio astronomy frequencies up to 1 THz are used.

Basic elements of such circuits are the transmission lines, whose propagation behavior has to be determined accurately. It can be calculated by applying Maxwellian equations to the infinitely long homogeneous transmission line structure and solving an eigenvalue problem [1], [2], [3], which is complex in general.

For numerical treatment, the computational domain has to be truncated by electric or magnetic walls or by a so-called absorbing boundary condition simulating open space. A very efficient formulation for the latter case is the Perfectly Matched Layer (PML). These layers consist of an artificial material with complex anisotropic material properties. We have chosen the formulation by Sacks et al. [4], because it works with the genuine Maxwellian equations opposite to the earlier proposal by Berenger [5], [6].

On each waveguide only a finite number of modes is to be considered. That is possible because the energy of the complex and evanescent modes decreases exponentially with the distance from any discontinuity. These modes can be neglected within the limit of accuracy. Only a finite number of modes is able to propagate and have to be taken into consideration.

2 Eigen Mode Problem

We start from the Maxwellian equations in frequency domain, written in integral form

$$\oint_{\partial\Omega} \vec{H} \cdot d\vec{s} = \int_{\Omega} \jmath\omega[\epsilon]\vec{E} \cdot d\vec{\Omega}, \qquad \oint_{\cup\Omega} ([\epsilon]\vec{E}) \cdot d\vec{\Omega} = 0, \tag{1}$$

$$\oint_{\partial\Omega} \vec{E} \cdot d\vec{s} = -\int_{\Omega} \jmath\omega[\mu]\vec{H} \cdot d\vec{\Omega}, \qquad \oint_{\cup\Omega} ([\mu]\vec{H}) \cdot d\vec{\Omega} = 0, \tag{2}$$

with the constitutive relations

$$\vec{D} = [\epsilon]\vec{E}, \quad \vec{B} = [\mu]\vec{H}. \tag{3}$$

The electric and the magnetic field intensities $\vec{E}$ and $\vec{H}$, and the electric and magnetic flux densities $\vec{D}$ and $\vec{B}$ are complex functions of the spatial coordinates. ω is the circular frequency of the sinusoidal excitation, and $\jmath^2 = -1$. The quantities $[\epsilon]$, $[\mu]$ (permittivity and permeability) are assumed to be diagonal complex tensors:

$$[\epsilon] = \mathrm{diag}\left(\epsilon_x, \epsilon_y, \epsilon_z\right), \quad [\mu] = \mathrm{diag}\left(\mu_x, \mu_y, \mu_z\right), \tag{4}$$

or complex scalars. The Maxwellian equations are discretized according to the Yee scheme [7] which consists of a primary and dual grid. Using the Finite Integration Technique (FIT) [8], [9], [10] with the lowest-order integration formulae

$$\oint_{\partial\Omega} \vec{f} \cdot d\vec{s} \approx \sum(\pm f_i s_i), \quad \int_{\Omega} \vec{f} \cdot d\vec{\Omega} \approx f\Omega \tag{5}$$

the Equations (1), (2) are transformed into a set of Maxwellian grid equations:

$$A^T D_{s/\mu} \vec{b} = \jmath\omega\epsilon_0\mu_0 D_{A_\epsilon} \vec{e}, \qquad B D_{A_\epsilon} \vec{e} = 0, \tag{6}$$

$$A D_s \vec{e} = -\jmath\omega D_{A_\mu} \vec{b}, \qquad B^T D_{A_\mu} \vec{b} = 0. \tag{7}$$

The vectors $\vec{e}$ and $\vec{b}$ contain the components of the electric field intensity and of the magnetic flux density of the elementary cells, respectively. A is defined as the operator of the line integral in the second Maxwellian equation (left formula of (2)) using the primary grid. B consists of 3 submatrices because

of homogeneity with the first Maxwellian equation. The submatrix of B is defined as the operator of the surface integral in Gauss' flux law (right formula of (1)) using the dual grid. A and B are sparse, and contain the values 1, -1, and 0 only. The diagonal matrices $D_{s/\mu}$, D_{A_ϵ}, D_s, and D_{A_μ} contain the information on cell dimension and material. ϵ_0 and μ_0 denote the permittivity and the permeability for the vacuum, respectively.

Eliminating the components of the magnetic flux density from the two equations of the left-hand side of (6), (7) we get the system of linear algebraic equations

$$(A^T D_{s/\mu} D_{A_\mu}^{-1} A D_s - k_0^2 D_{A_\epsilon})\vec{e} = 0, \quad k_0 = \omega\sqrt{\epsilon_0 \mu_0}, \tag{8}$$

which have to be solved using the boundary conditions. k_0 is the wavenumber in vacuo.

The transverse electric mode fields at the ports have to be computed before the system of linear equations (8) can be solved. Because the transmission lines are longitudinally homogeneous any field can be expanded into a sum of so-called modal fields which vary exponentially in the longitudinal direction:

$$\vec{E}(x, y, z \pm 2h) = \vec{E}(x, y, z) e^{\mp \jmath k_z 2h}. \tag{9}$$

A substitution of ansatz (9) into the system of linear algebraic equations (8) and the elimination of the longitudinal electric field intensity components by means of the electric-field divergence equation $BD_{A_\epsilon}\vec{e} = 0$ (see (6)) gives an eigenvalue problem:

$$C\underline{\vec{e}} = \gamma\underline{\vec{e}}, \quad \gamma = -4\sin^2(hk_z) \approx -4(hk_z)^2 = u + \jmath v. \tag{10}$$

$\underline{\vec{e}}$ consists of components $E_{x_{i,j,k}}$ and $E_{y_{i,j,k}}$, of the eigenfunctions. The order of C is $2n_x n_y - n_b$. $n_x n_y$ is the number of elementary cells at the port. The size of n_b depends on the number of cells with perfectly conducting material. $2h$ is the length of an elementary cell in z-direction. The sparse matrix C is in general nonsymmetric complex, or nonsymmetric real for lossless structures. The problem for the transmission line is reduced to a two dimensional problem. We can use the approximation $\sin(x) \approx x$ in (10) if we choose h small enough, which is necessary anyway to get small discretization errors. $k_z = \beta - \jmath\alpha$ is the propagation constant. A propagation constant k_z and its corresponding eigenfunction is called a mode. The relation between

the propagation constants k_z and the eigenvalues γ is nonlinear:

$$k_z = \frac{\jmath}{2h} \ln\left(\frac{\gamma}{2} + 1 + \sqrt{\frac{\gamma}{2}\left(\frac{\gamma}{2} + 2\right)}\right) = \beta - \jmath\alpha. \tag{11}$$

The energy of the complex and evanescent modes decreases exponentially with the distance from the discontinuity. In technical applications most of the modes can be neglected within the limit of accuracy. Only a finite number of modes is able to propagate and have to be taken into consideration. These are the modes with the smallest magnitude of imaginary part, but possibly with large real part. Therefore, to sort the propagation constants according to their importance in our problem, we use the
Criterion: The propagation constants k_z are sorted in ascending order of $|\alpha|$. In the case that some $|\alpha|$ have the same value the constants k_z are sorted in descending order of $|\beta|$.

3 Maximum Propagation Constant

For our method we need an estimation of the maximum of $\Re(k_z)$, the real part of the propagation constants of the waveguide. We get it in the following way.

For simplicity we suppose the materials of the waveguide, contrary to the PML layers, to be isotropic, which is true in most practical cases. That means

$$\epsilon = \epsilon_x = \epsilon_y = \epsilon_z, \quad \mu = \mu_x = \mu_y = \mu_z. \tag{12}$$

We compare k_z with the wave vector $\vec{k}$ of plane waves in an unbounded homogeneous medium with permittivity ϵ and permeability μ. Plane waves are described by

$$\vec{E} = \vec{E}_0 e^{\jmath(\omega t - \vec{k}\cdot\vec{r})} \tag{13}$$

with the dispersion relation

$$k = \sqrt{\vec{k}\cdot\vec{k}} = \omega\sqrt{\epsilon\mu}. \tag{14}$$

Separation of real and imaginary part yields

$$\Re(k) = \omega\sqrt{\frac{1}{2}\left(\Re(\epsilon\mu) + \sqrt{(\Re(\epsilon\mu))^2 + (\Im(\epsilon\mu))^2}\right)} \tag{15}$$

and

$$\Im(k) = -\omega\sqrt{\frac{1}{2}\left(-\Re(\epsilon\mu) + \sqrt{(\Re(\epsilon\mu))^2 + (\Im(\epsilon\mu))^2}\right)} \tag{16}$$

with

$$\Re(\epsilon\mu) = \Re(\epsilon)\Re(\mu) - \Im(\epsilon)\Im(\mu), \quad \Im(\epsilon\mu) = \Im(\epsilon)\Re(\mu) + \Im(\mu)\Re(\epsilon). \tag{17}$$

In a lossless waveguide homogeneously filled with the same material we have $k_z \leq k$. Therefore, in the case of a waveguide filled with several different and lossy materials we could use as an estimation of the upper limit of $\Re(k_z)$ the expression

$$k_f = \omega\sqrt{\frac{1}{2}\left(\Re(\epsilon_m\mu_m) + \sqrt{(\Re(\epsilon_m\mu_m))^2 + (\Im(\epsilon_m\mu_m))^2}\right)}, \tag{18}$$

where ϵ_m and μ_m refer to the material that yields the largest value of $\Re(k)$. This value will be unnecessarily high, however, if some of the materials are metals. Metals have very large values of $|\Im(\epsilon)|$ and therefore large $\Re(k)$. But for the same reason also $\Im(k)$ will be large so that electromagnetic waves are strongly attenuated in metals. As we are interested in propagating modes, we can exclude all metals from the search for ϵ_m and μ_m. The border between metals and lossy dielectrics is somewhat arbitrary, but can be defined for instance by

$$\text{metals:} \quad |\Im(\epsilon)| > \lambda|\Re(\epsilon)|, \qquad \text{lossy dielectrics:} \quad |\Im(\epsilon)| \leq \lambda|\Re(\epsilon)| \tag{19}$$

with λ in the order of 10^2.

The PML layers can also be excluded from the search for ϵ_m and μ_m, because the electromagnetic fields of propagating modes are concentrated in the area of the waveguide (see chapter 5).

4 Computation of the Propagation Constants

We use the implicitly restarted Arnoldi method [11], [12] to calculate the eigenvalues. The Arnoldi method has to be carried out twice in order to avoid the computation of all eigenvalues but to find the few first propagation constants according to the above formulated criterion.

In general the Arnoldi method does not converge using the regular mode for our eigenvalue problem. Thus, the Arnoldi algorithm is called iteratively to solve the standard eigenvalue problem using the inverse mode $C^{-1}x = \frac{1}{\gamma}x$ with the solution of systems of linear algebraic equations. The eigenvalue problem has to be solved with high accuracy. It is ill-conditioned. Thus, we have chosen a direct method for the solution of the systems of linear algebraic equations. We use a combined unifrontal/multifrontal method [13] for the solution of large sparse sets of ill-conditioned nonsymmetric complex linear algebraic equations.

By means of the Arnoldi iteration we can compute a set of eigenvalues of largest or smallest magnitude, real part or imaginary part, but we cannot find in one step the set of eigenvalues according to our criterion. Therefore, we must proceed in two steps.

We discuss the two steps.
First we calculate a subset of m_1 eigenvalues $\gamma_i = u_i + v_i$ of smallest magnitude. These eigenvalues are located in the circle C_1 of the γ-plane of radius r_1 and centered at the origin (see Figure 2). To find these values we use the Arnoldi method in inverse mode looking for eigenvalues of largest magnitude. These values are located outside of the circle C'_1 in the γ^{-1}-plane (see Figure 3). We are interested in the corresponding propagation constants. These are located in the circle $\hat{C}_1$ (see Figure 4) of the k_z-plane.

To make the Figures 2, 3, and 4 more understandable the relations between these three planes are given in the Tables 1, 2, and 3 in the Appendix.

We have to find a set of propagation constants with the smallest magnitude of the imaginary part, but possibly with large real part. Generally the eigenvalues which correspond with these propagation constants do not belong to the subset of eigenvalues of smallest magnitude, computed in the first step.

How can we find the wanted eigenvalues?
To search for the corresponding additional eigenvalues, we use a second run of the Arnoldi method with a modified matrix.

The wavenumber k_f is an upper bound for the interesting propagation constants of undamped modes in a waveguide. Using the estimation of the square of the maximum wavenumber of the cells (18) we find the estimation (see also (10))

$$\gamma^{(max)} \approx -4\,(hk_f)^2 \tag{20}$$

of the maximum interesting eigenvalue.
Because of (see (10) and (11))

$$\gamma \approx -4(hk_z)^2 = -4\left((h\beta)^2 - (h\alpha)^2\right) + 8\jmath h^2\alpha\beta \tag{21}$$

we can distinguish the two cases

$$\begin{array}{lrcl} \text{(a)} & \Re(\gamma) & = & -4h^2(\beta^2-\alpha^2) < 0 \Rightarrow \beta^2 > \alpha^2, \\ \text{(b)} & \Re(\gamma) & = & -4h^2(\beta^2-\alpha^2) > 0 \Rightarrow \beta^2 < \alpha^2. \end{array} \tag{22}$$

In the case (b), the magnitudes of the imaginary parts of the propagation constants, which are not computed, are greater than the magnitudes of the imaginary parts of the intersections points of the curve $\hat{C}_1$ with $\alpha = \beta$ or $\alpha = -\beta$ (see Figure 4). That means, we have to search only additional propagation constants which correspond with eigenvalues with negative real parts (case (a)). Thus, we extend the matrix C (see (10)) by a diagonal matrix

$$\Gamma = \mathrm{diag}(\gamma_1, \cdots, \gamma_{m_a}), \tag{23}$$

which consists of the set $\mathcal{E}^{(a)}$ of m_a negative elements:

$$\gamma_\tau = r_3\left(1 + \frac{\tau - 1}{100}\right), \quad \tau = 1(1)m_a, \qquad r_3 = \frac{5}{4}r_2, \quad r_2 = \frac{\gamma^{(max)}}{2}. \tag{24}$$

Now we compute a subset $\mathcal{E}^{(l)}$ of $m_a + m_r$ eigenvalues of smallest real part of the extended matrix

$$\bar{C} = \begin{pmatrix} \Gamma & \\ & C \end{pmatrix} \tag{25}$$

using the Arnoldi method in inverse mode. m_r is the number of eigenvalues with negative real parts calculated during the first run. Eigenvalues of C which fulfill the condition "smallest real part" belong to $\mathcal{E}^{(l)}$ rather than the eigenvalues of $\mathcal{E}^{(a)}$, and we can separate the m_n new eigenvalues from the set $\mathcal{E}^{(l)}$. If $m_n = m_a$ we have to reiterate the second run with a greater m_a. Otherwise, it could be that we have not found all eigenvalues of smallest real part greater than γ_{m_a}.
The reciprocal eigenvalues computed in this second run are located left from the vertical line C_4' in the γ^{-1}-plane (see Figure 3). The corresponding eigenvalues are located in the circle C_4 in the γ-plane of radius r_4 centered at the

negative u-axis and touching the v-axis (see Figure 2). The corresponding propagation constants are located in the k_z-plane inside of the lemniscate $\hat{C}_4$ (see Figure 4).

We use the radius r_3 rather than r_2 (see (24) and Figures 2, 3, and 4) because propagation constants which correspond with eigenvalues, which are located in the area *hab* of the γ-plane, could have any small imaginary parts (see area $\hat{h}\hat{a}\hat{b}$ of the k_z-plane). Finally we use the radius r_4 rather than r_3 because the eigenvalues $\gamma_\tau, \tau = 1(1)m_a$, are located left from $u = -2r_3$ (see Table 1, (24), and Figure 2).

All propagation constants, which are not computed, are located outside of $\hat{C}_1$ and $\hat{C}_4$, and their smallest imaginary part can be controled by r_1, r_2 and r_4 (see Table 1). We consider the points of intersections of the lemniscate $\hat{C}_4$ with the circle $\hat{C}_1$ and with the hyperbola $\hat{V}_1$ (see Figure 4 and Table 4). The intersection points with the smallest magnitude of the imaginary part specify the strip (denoted by α_{min} and $-\alpha_{min}$ in Figure 4) which contains all propagation constants with a magnitude of imaginary part less than the minimum value α_{min}.

We note, it is essential not to demand more eigenvalues of smallest real part of $\bar{C}$ than eigenvalues with negative real parts of $\bar{C}$ exist, because the Arnoldi method does not converge for our problem in this case.

We note, the factorization of the sparse extended matrix $\bar{C}$ (see (25)) is obviously a modification of the factorization of C (see (10)), i.e., we can avoid a second matrix factorization.

We note, a second run is dispensable if the circle $\hat{C}_1$ includes the lemniscate $\hat{C}_4$.

5 PML-Modes

In the analytic formulation, the interface between a normal medium and a Perfectly Matched Layer is exactly reflectionless. Any incident wave penetrates the PML, will be attenuated and reaches the outer surface, where it strikes an electric wall. Here the wave is reflected and re-enters the waveguide after a second traversing of the PML. In order to keep the amplitude of the re-entering wave small enough, the PML must have a certain thickness. The finite volume of the PML introduces additional modes that are not an intrinsic property of the waveguide. We want to exclude these modes from

the output of the programme. The PML-modes can be characterized by their high power concentration in the PML. Thus, to eliminate the PML-modes we compute the magnitude of the power flow of every computed mode in the PML (P^{PML}) and in the total computational domain (P):

$$P = P^{(PML)} + P^{(CD)} = \int\limits_{\Omega^{(PML)}} (\vec{E}_t \times \vec{H}^*_{t,m}) \cdot d\vec{\Omega} + \int\limits_{\Omega^{(CD)}} (\vec{E}_t \times \vec{H}^*_{t,m}) \cdot d\vec{\Omega} \ . \tag{26}$$

A mode is accepted as a "normal" mode if

$$r^{(CD)} = \frac{P^{(CD)}}{P} > 0.6 \ , \tag{27}$$

where the number 0.6 was found empirically.

6 Numerical Example

As an example we have calculated the propagation constants and the mode fields of a coplanar waveguide (see Figure 1). The computational domain consists of the cross section of the waveguide, surrounded by the PML region, and magnetic and electric walls. As the waveguide is symmetrical, only its right-hand half must be discretized. The magnetic wall acts as a symmetry plane. The structure is subdivided into $n_{xy} = n_x n_y$ elementary cells, $n_x = 91$, $n_y = 62$, including a 22-cell PML region. We remark that theoretically one sufficiently thick layer surrounding the waveguide domain can absorb without reflections any kind of wave travelling towards boundaries. In the discretized version, however, the PML region has to contain enough cells in order to approximate the decay of the penetrating waves. Otherwise the waveguide-PML interface would give rise to numerical reflection. The dimension of the eigenvalue problem is $2n_x n_y - n_b = 10674$. n_b is determinated by the number of cells filled with perfectly conducting material. $m_1 = 6$ eigenvalues computed in the first run are located in C_1 (see grey dots in Figure 2). The corresponding propagation constants are located in the circle $\hat{C}_1$ (see grey dots in Figure 4). The matrix C was extended by $m_a = 15$ negative elements. The propagation constants calculated in the second run are located in the lemniscate $\hat{C}_4$ (see black dots in Figure 4). We see, the magnitude of the imaginary part of some propagation constants computed in the second run is

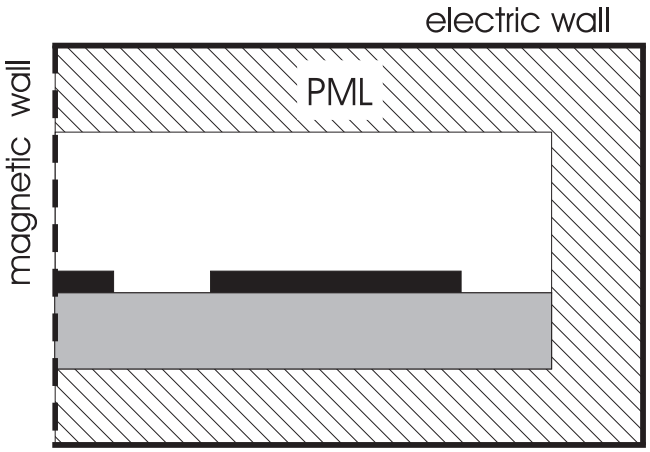

Figure 1: Cross section of a coplanar waveguide (not to scale)

less than the magnitude of the imaginary parts of the first run. These modes would not have been found by the one-step-method.

7 Appendix

The mapping relations between the γ- and the γ^{-1}-plane (inversion) are

$$\begin{array}{lllllll} \gamma & = & u + \jmath v, & \gamma & = & \frac{1}{z}, & z = x + \jmath y, \\ u & = & \frac{x}{x^2+y^2}, & v & = & -\frac{y}{x^2+y^2} \ . \end{array} \tag{28}$$

The eigenvalues in the γ-plane are mapped into the propagation constants in the k_z-plane:

$$\begin{array}{lllllll} \gamma & = & u + \jmath v, & \gamma & = & -4(hk_z)^2, & k_z = \beta - \jmath\alpha, \\ u & = & -4h^2(\beta^2 - \alpha^2), & v & = & 8h^2\alpha\beta. & \end{array} \tag{29}$$

Our immediate purpose is to see how lines or areas map from one plane to another. The Tables 1, 2, 3, and 4 contain the functions and points which are visualized in the Figures 2, 3, and 4.

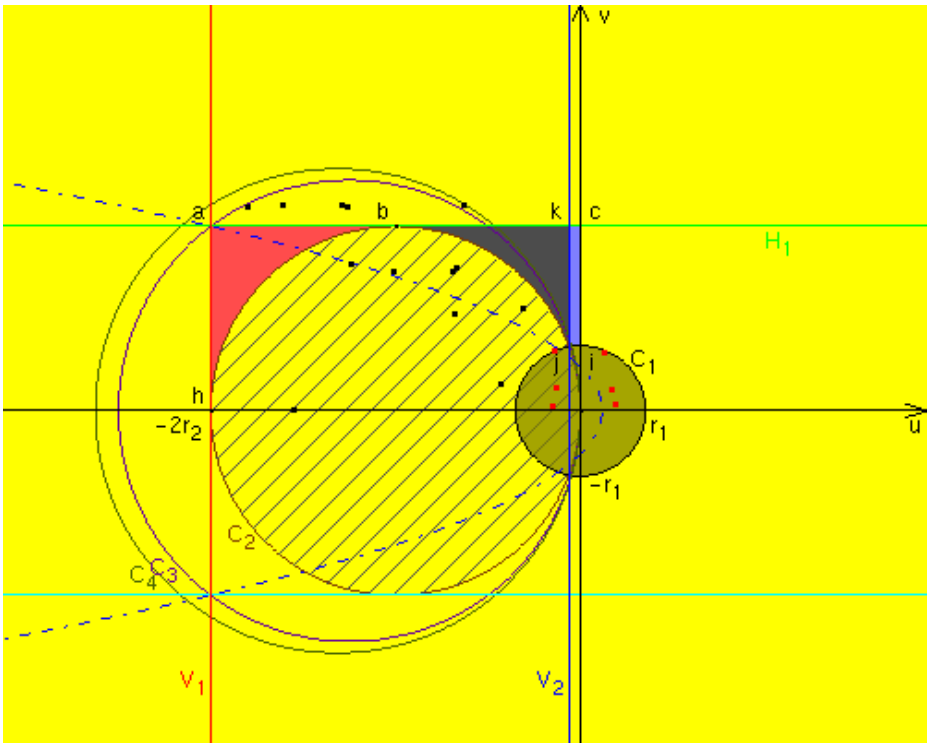

Figure 2: γ-plane

$C_1:$	u^2+v^2	$=$		$r_1{}^2,$	$r_1 = \max\limits_{i=1,m_1}\left\{\sqrt{u_i^2+v_i^2}\right\},$ circle
$C_2:$	$(u+r_2)^2+v^2$	$=$		$r_2^2,$	$r_2 = \frac{\gamma^{(max)}}{2},$ circle
$C_3:$	$(u+r_3)^2+v^2$	$=$		$r_3^2,$	$r_3 = \frac{5}{4}r_2,$ circle
$C_4:$	$(u+r_4)^2+v^2$	$=$		$r_4^2,$	$r_4 = \frac{\gamma_{m_a}}{2},$ circle
$H_1:$	v	$=$		$r_2,$	horizontal straight line
$V_1:$	u	$=$	$-$	$2r_2,$	vertical straight line
$V_2:$	u	$=$		$u_j,$	vertical straight line

Table 1: Functions of the curves in the γ-plane

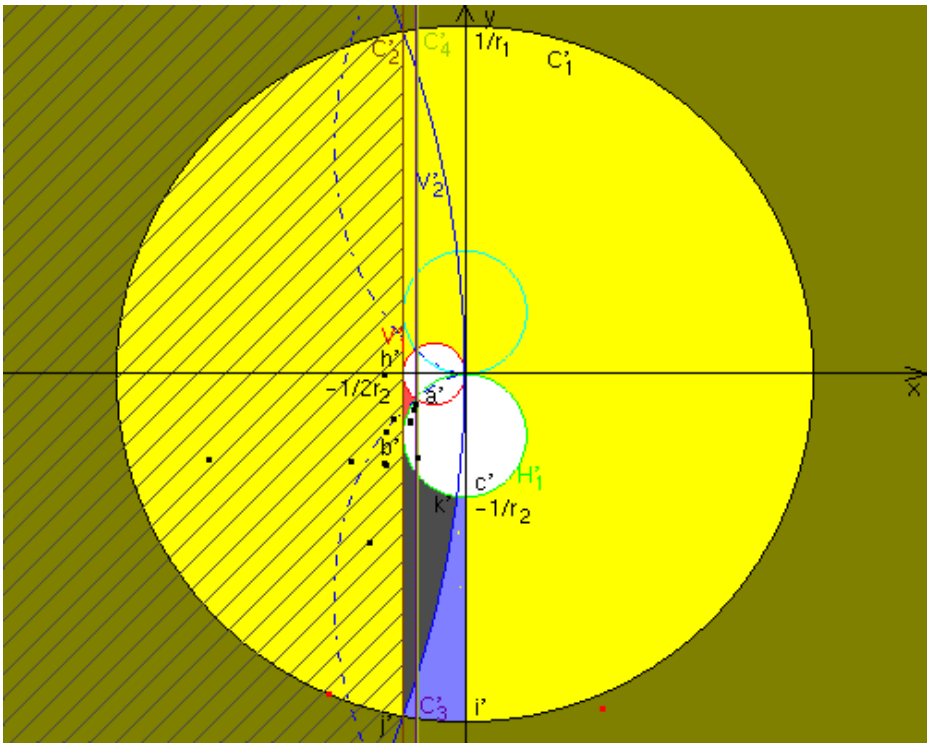

Figure 3: γ^{-1}-plane

C'_1 :	x^2+y^2	$=$	$\left(\frac{1}{r_1}\right)^2$,	circle
C'_2 :	x	$=$	$-\frac{1}{2r_2}$,	vertical straight line
C'_3 :	x	$=$	$-\frac{1}{2r_3}$,	vertical straight line
C'_4 :	x	$=$	$-\frac{1}{2r_4}$,	vertical straight line
H'_1 :	$x^2+\left(y+\frac{1}{2r_2}\right)^2$	$=$	$\left(\frac{1}{2r_2}\right)^2$,	circle
V'_1 :	$\left(x+\frac{1}{4r_2}\right)^2+y^2$	$=$	$\left(\frac{1}{4r_2}\right)^2$,	circle
V'_2 :	$\left(x-\frac{1}{2u_j}\right)^2+y^2$	$=$	$\left(\frac{1}{2u_j}\right)^2$,	circle

Table 2: Functions of the curves in the γ^{-1}-plane

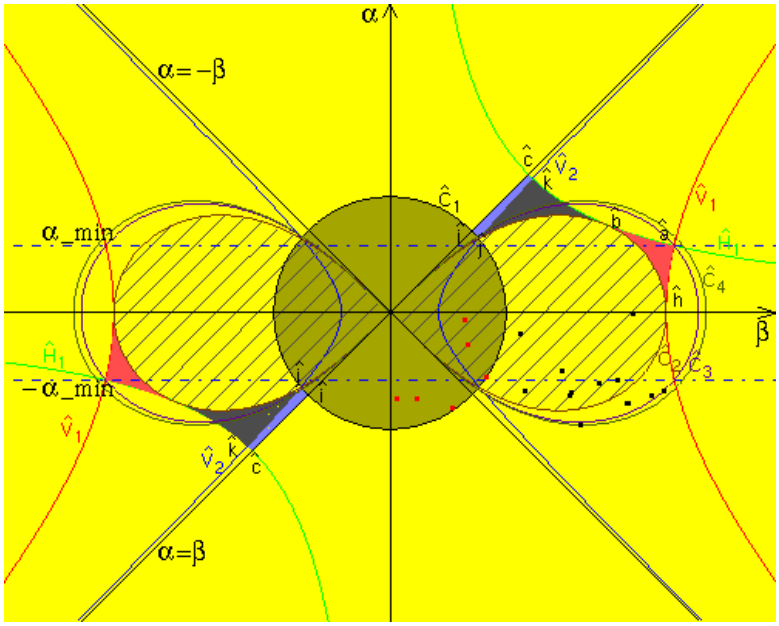

Figure 4: k_z-plane

$\hat{C}_1$:	$\beta^2+\alpha^2$	$=$		$\frac{r_1}{4h^2}$,	circle
$\hat{C}_2$:	$(\beta^2+\alpha^2)^2-\frac{r_2}{2h^2}(\beta^2-\alpha^2)$	$=$		0,	lemniscate
$\hat{C}_3$:	$(\beta^2+\alpha^2)^2-\frac{r_3}{2h^2}(\beta^2-\alpha^2)$	$=$		0,	lemniscate
$\hat{C}_4$:	$(\beta^2+\alpha^2)^2-\frac{r_4}{2h^2}(\beta^2-\alpha^2)$	$=$		0,	lemniscate
$\hat{H}_1$:	$\alpha\beta$	$=$		$\frac{r_2}{8h^2}$,	hyperbola
$\hat{V}_1$:	$\beta^2-\alpha^2$	$=$		$\frac{r_2}{2h^2}$,	hyperbola
$\hat{V}_2$:	$\beta^2-\alpha^2$	$=$	$-$	$\frac{u_j}{4h^2}$,	hyperbola

Table 3: Functions of the curves in the k_z-plane

$\hat{C}_4, \hat{C}_1$:	$(\beta_{\hat{j}_4}, \alpha_{\hat{j}_4})$	$=$	$\left(\pm\frac{1}{4h}\sqrt{\frac{r_1}{r_4}(2r_4+r_1)}, \pm\frac{1}{4h}\sqrt{\frac{r_1}{r_4}(2r_4-r_1)}\right)$
$\hat{C}_4, \hat{V}_1$:	$(\beta_{\hat{a}_4}, \alpha_{\hat{a}_4})$	$=$	$\left(\pm\frac{1}{2h}\sqrt{\sqrt{r_2 r_4}+r_2}, \pm\frac{1}{2h}\sqrt{\sqrt{r_2 r_4}-r_2}\right)$

Table 4: Intersection points in the k_z-plane

References

[1] A. Christ and H. L. Hartnagel. Three-dimensional finite-difference method for the analysis of microwave-device embedding. *IEEE Transactions on Microwave Theory and Techniques*, MTT-35, No. 8:688–696, June 1987.

[2] A. Christ. Streumatrixberechnung mit dreidimensionalen Finite-Differenzen für Mikrowellen-Chip-Verbindungen und deren CAD-Modelle. *Fortschrittberichte VDI, Reihe 21: Elektrotechnik*, Nr. 31:1–154, 1988.

[3] G. Hebermehl, R. Schlundt, H. Zscheile, and W. Heinrich. Eigen mode solver for microwave transmission lines. *The International Journal for Computation and Mathematics in Electrical and Electronic Engineering*, 16, No. 2:108–122, 1997.

[4] Z.S. Sacks, D.M. Kingsland, R. Lee, and J.-F. Lee. A perfectly matched anisotropic absorber for use as an absorbing boundary condition. *IEEE Transactions on Antennas and Propagation*, 43, No. 12:1460–1463, December 1995.

[5] J.-P. Berenger. Perfectly matched layer for the absorption of electromagnetic waves. *Journal for Computational Physics*, 114:185–200, 1994.

[6] J.-P. Berenger. Improved PML for the FDTD solution of wave-structure interaction problems. *IEEE Transactions on Antennas and Propagation*, 45, No. 3:466–473, March 1997.

[7] K. Yee. Numerical solution of initial boundary value problems involving Maxwell's equations in isotropic media. *IEEE Transactions on Antennas and Propagation*, AP-14, No. 3:302–307, May 1966.

[8] T. Weiland. A discretization method for the solution of Maxwell's equations for six-component fields. *Electronics and Communication (AEÜ)*, 31:1–116, 1977.

[9] K. Beilenhoff, W. Heinrich, and H. L. Hartnagel. Improved finite-difference formulation in frequency domain for three-dimensional scattering problems. *IEEE Transactions on Microwave Theory and Techniques*, 40, No. 3:540–546, March 1992.

[10] G. Hebermehl, R. Schlundt, H. Zscheile, and W. Heinrich. Improved numerical methods for the simulation of microwave circuits. Preprint No. 467, Weierstraß-Institut für Angewandte Analysis und Stochastik im Forschungsverbund Berlin e.V., 1998. 1–18, to appear in: Surveys on Mathematics for Industry.

[11] D. C. Sorensen. Implicit application of polynomial filters in a k-step Arnoldi method. *SIAM J. Matr. Anal. Apps.*, 13:357–385, 1992.

[12] R. B. Lehoucq. Analysis and implementation of an implicitly restarted Arnoldi iteration. Technical Report TR95-13, Rice University, Department of Computational and Applied Mathematics, 1995.

[13] T. A. Davis and I. S. Duff. A combined unifrontal/multifrontal method for unsymmetric sparse matrices. Report TR97-016, University of Florida, 1997.